01 Jan 2015

Computational Discovery of Lanthanide Doped and Co-Doped $Y_3Al_5O_{12}$ for Optoelectronic Applications

Kamal Kumar Choudhary

Aleksandr V. Chernatynskiy
Missouri University of Science and Technology, aleksandrc@mst.edu

Kiran Mathew

Eric W. Bucholz

et. al. For a complete list of authors, see https://scholarsmine.mst.edu/phys_facwork/440

Recommended Citation

K. K. Choudhary et al., "Computational Discovery of Lanthanide Doped and Co-Doped $Y_3Al_5O_{12}$ for Optoelectronic Applications," *Applied Physics Letters*, vol. 107, no. 11, American Institute of Physics (AIP), Jan 2015.
The definitive version is available at https://doi.org/10.1063/1.4929434

Computational discovery of lanthanide doped and Co-doped $Y_3Al_5O_{12}$ for optoelectronic applications

Kamal Choudhary,[1] Aleksandr Chernatynskiy,[1] Kiran Mathew,[2] Eric W. Bucholz,[3] Simon R. Phillpot,[1] Susan B. Sinnott,[1] and Richard G. Hennig[1,2]
[1]*Department of Materials Science and Engineering, University of Florida, Gainesville, Florida 32611-6400, USA*
[2]*Department of Materials Science and Engineering, Cornell University, Ithaca, New York 14853, USA*
[3]*Department of Materials Science and Engineering, North Carolina State University, Raleigh, North Carolina 27695-7907, USA*

(Received 20 May 2015; accepted 12 August 2015; published online 18 September 2015)

We systematically elucidate the optoelectronic properties of rare-earth doped and Ce co-doped yttrium aluminum garnet (YAG) using hybrid exchange-correlation functional based density functional theory. The predicted optical transitions agree with the experimental observations for single doped Ce:YAG, Pr:YAG, and co-doped Er,Ce:YAG. We find that co-doping of Ce-doped YAG with any lanthanide except Eu and Lu lowers the transition energies; we attribute this behavior to the lanthanide-induced change in bonding environment of the dopant atoms. Furthermore, we find infrared transitions only in case of the Er, Tb, and Tm co-doped Ce:YAG and suggest Tm,Ce:YAG and Tb,Ce:YAG as possible functional materials for efficient spectral up-conversion devices. [http://dx.doi.org/10.1063/1.4929434]

Lanthanide (Ln) doped and co-doped yttrium aluminum garnet (YAG) has a wide range of applications including light emitting diodes (LED),[1] lasers,[2] phosphors,[3] infrared pressure sensors,[4] and spectral convertors for improving solar cell performance.[5,6] Among these, spectral conversion has recently received increased attention,[5,7] with YAG-based materials such as Ce:YAG and Er:YAG[8] having high quantum efficiency. Interestingly, experimental efforts to co-dope Er:YAG with Ce have resulted in an increase in the quantum efficiency via enhanced infrared optical absorption. However, there is still a strong need for even higher quantum efficiency materials,[5,7] for which a better understanding of the governing optoelectronic phenomenon is required.

Recent, density-functional theory (DFT) calculations with semi-local exchange-correlation functionals revealed the atomic and electronic structure as well as optical transition characteristics for pure YAG,[9] Ce-La:YAG,[10] and Cr:YAG.[11] However, the semi-local exchange-correlation functionals used are problematic because they underestimate the band gap and predict an incorrect position of the *f*-states of the lanthanides.[9,10,12–14] Improved approximations to DFT, such as nonlocal hybrid functionals,[15] and many-body approaches, such as the GW approximation,[16] are generally more accurate for electronic structure than semi-local exchange-correlation functionals. Thus, there is a need to apply these methods to address the drawbacks of conventional DFT and to develop the systematics in optoelectronic properties trends that can be used to optimize performance of materials.

In this letter, we determine the optoelectronic properties of lanthanide doped and co-doped Ln:YAG using the Heyd-Scuseria-Ernzerhof hybrid functional (HSE06),[17] which establishes an accurate description of the electronic properties of materials[18] at a reasonable computational cost. We find through comparison with experimental values that the band-gap and the frequency dependent dielectric function of the undoped YAG host material as well as the defect levels and optical transitions of the Ln-doped YAG are well described by the HSE06 functional. We also find that the co-doping of Ce-doped YAG with any lanthanide except Eu and Lu lowers the energy of the optical transitions.[19] We compare materials based on presence of low energy infrared peaks, which are again related to the quantum efficiency of devices. To understand the origin of the change in optical transition energy in Ce co-doped systems compared to Ce:YAG, we characterize the charge and bonding environment of the dopant atoms. We attribute the spectral shift in the co-doped materials to the volume change induced by the Ln atoms. We predict that co-doping with Tb and Tm results in infrared optical transitions, making Tm,Ce:YAG and Tb,Ce:YAG candidate functional materials for efficient spectral up-conversion devices.

The DFT calculations are performed using the Vienna *Ab-initio* Simulation Package (VASP)[20] and the projector-augmented wave (PAW) method.[21] The doping is modeled by substituting a lanthanide for an yttrium atom in a 160-atom cubic simulation cell of YAG with a chemical formula $Y_{(3-x)}Ln_xAl_5O_{12}$ ($x = 0.125$). This concentration lies approximately in the middle of the range of experimental concentrations: $x = 0.03$ to 0.3.[22] The Ce co-doped system is considered with an effective composition of $Y_{2.75}Ce_{0.125}Ln_{0.125}Al_5O_{12}$. For the co-doped system, the distance between Ce and Ln is taken as 7.06 Å. Previous DFT calculations[23] show that the total energy shift with respect to the distance between Ce and Ln is in the range of meV, which is very small. The calculations are done in two steps: First, the atomic structure is optimized using the semi-local exchange-correlation functional by Perdew, Burke, and Ernzerhof (PBE).[24] Second, the electronic structure is calculated using the HSE06 exchange-correlation functional.[17] The inclusion of 25% of exact exchange for short distances in the HSE06 functional improves the band gap by recovering the derivative

discontinuity of the Kohn-Sham potential for integer electron numbers.[25] The orbitals are expanded in a plane-wave basis with an energy cutoff of 400 eV. A $4\times4\times4$ k-point mesh is used for the Brillouin zone integration for the PBE functional and the Γ point for the computationally more demanding HSE06 functional.

To obtain the optical properties of the doped materials, we calculate the imaginary part of the dielectric function from the Bloch wavefunctions and eigenvalues[26]

$$\varepsilon_{\alpha\beta}(\omega) = \frac{4\pi^2e^2}{\Omega}\lim_{q\to0}\frac{1}{q^2}\sum_{c,v,k}2w_{\vec{k}}\delta(\zeta_{ck}-\zeta_{vk}-\omega) \times \langle\psi_{c\vec{k}+\vec{e}_\alpha q}|\psi_{v\vec{k}}\rangle\langle\psi_{c\vec{k}+\vec{e}_\beta q}|\psi_{v\vec{k}}\rangle^*, \quad (1)$$

where e is electron charge, Ω is the cell volume, $w_{\vec{k}}$ is the Fermi-weight of each k-point, $\vec{e}_\alpha$ are unit vectors along the three Cartesian directions, $|\psi_{n\vec{k}}\rangle$ is the cell-periodic part of the Bloch orbital for band n and k-point $\vec{k}$, q stands for the wave vector of an incident photon, c and v stand for conduction and valence bands, and ζ stands for eigenvalues of the corresponding bands respectively. The matrix elements on the right side of Eq. (1) capture the transitions allowed by symmetry and selection rules.[27] Furthermore, the energy conservation described by the δ-function is usually approximated by a Gaussian-type smearing function for numerical reasons. However, this smearing makes it difficult to resolve the specific transitions due to the lanthanide dopants in the dielectric function. We therefore calculate directly the transition strength[11] for the Bloch wavefunctions and plot it against the energy $(\zeta_{ck}-\zeta_{vk})$ at the Γ point

$$\eta_{\alpha\beta,cv} = \frac{8\pi^2e^2}{\Omega}\lim_{q\to0}\frac{1}{q^2}\langle\psi_{c\vec{k}+\vec{e}_\alpha q}|\psi_{v\vec{k}}\rangle\langle\psi_{c\vec{k}+\vec{e}_\beta q}|\psi_{v\vec{k}}\rangle^*. \quad (2)$$

Based on the transition strength spectrum, we identify the various transitions that are induced by the presence of the dopants in the material.

For pure YAG, the lattice constant obtained is 11.99 Å, within 1% of the experimental value of 12.02 Å (Refs. 13 and 14) using PBE. The volumes of the doped Ln:YAG systems decrease along the lanthanide row (see Fig. S1 in the supplementary material[35]), following the well-known "lanthanide contraction" of decreasing ionic radii along the row.[28] Furthermore, the elastic constants obtained using density functional perturbation theory for YAG are $C_{11}=329$ GPa, $C_{12}=113$ GPa, and $C_{44}=109$ GPa, which agree closely with the experimental values of 339, 114, and 116 GPa, respectively.[29] This confirms that the PBE functional is well suited for the structural and mechanical properties of YAG.

Next, we assess the electronic and optical properties of pure YAG obtained from the PBE and HSE06 functional to establish the accuracy of our approach. Fig. 1(a) shows that the PBE functional predicts a band-gap for pure YAG of 4.6 eV underestimating the experimental value of 6.4 eV.

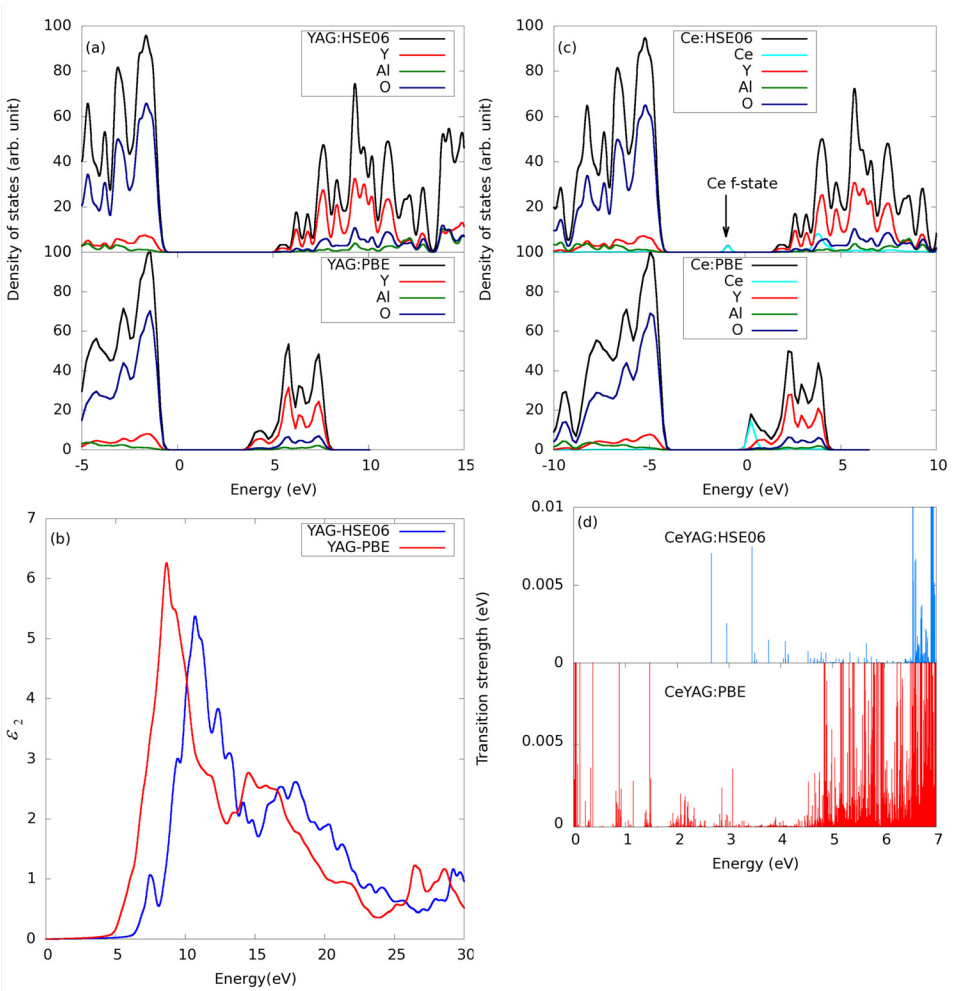

FIG. 1. (a) The projected density of states for pure YAG using the PBE and HSE06 functional shows that HSE06 predicts a band gap in agreement with experiments. (b) The dielectric function for pure YAG using PBE and HSE06. (c) The projected density of states for Ce-doped YAG shows that the Ce-d and f-states are located inside the gap-region of YAG using HSE06. (d) All possible transitions near the band-gap show that HSE06 reproduces the experimental emission wavelength for Ce:YAG. The Fermi energy is set to zero for density of states plot.

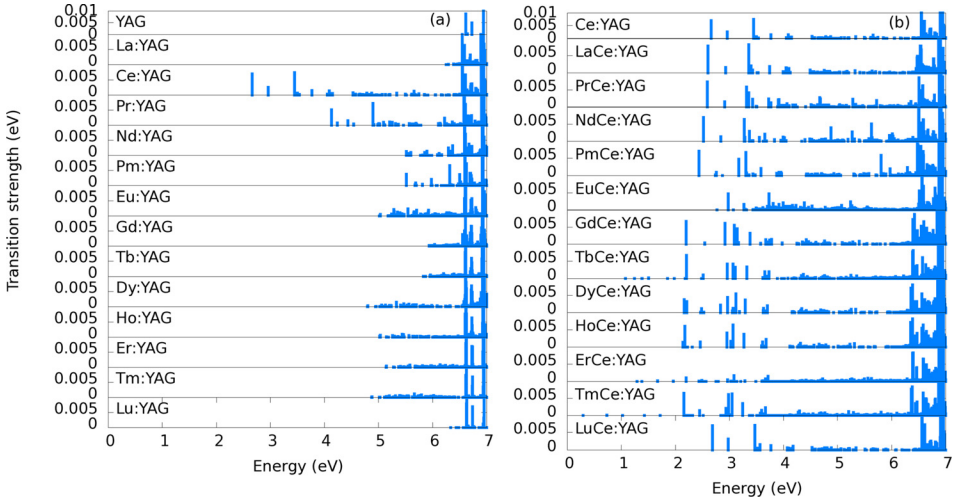

FIG. 2. (a) Transition strengths calculated using Eq. (2) are shown for all lanthanides. Peaks at 2.6 eV of Ce and 4.13 eV of Pr are comparable to experiments. (b) Transitions near visible spectrum for co-doped systems. For co-doping of Ce with other lanthanides, a blue shift is observed for Eu and Lu, while a red shift is observed for other lanthanides.

The HSE06 functional on the other hands predicts a value of 6.2 eV, in good agreement with experiment. The projected density of states (PDOS) shows that the conduction band is dominated by the yttrium *d*-states, while the valence band is dominated by the oxygen 2*p* states, in agreement with electron-loss near-edge spectroscopy (see Fig. 5 of Ref. 30).

Figure 1(b) shows the imaginary part of the dielectric function for pure YAG, which agrees well with the measurements by Tomiki *et al.*[14,31] The overall shape of the dielectric function for the PBE and HSE06 functional are very similar. However, the peak positions are shifted by the underestimated band-gap energy in PBE.

We also verify the electronic and optical properties of the Ce doped YAG. Figure 1(c) shows that for Ce:YAG, the *f*-states of Ce are outside the band-gap region with PBE, which is inconsistent with experiments.[32] On the other hand, with the HSE06 functional, the Ce *f*-states are located in the gap region of YAG. The transitions strengths, η, for Ce:YAG using PBE and HSE06 are presented in Fig. 1(d). The PBE functional displays various unphysical transitions at low energies, while the HSE06 functional shows a first peak at 2.66 eV in close agreement with the experimental value of 2.7 eV.[33]

It is important to note that while hybrid functionals can provide good estimates of the band edge positions and defect levels, they do not describe the excitonic effect, which requires computationally demanding many-body methods such as the Bethe-Salpeter equation. In this work, we focus on the optical transitions introduced through doping, i.e., the defect levels, which are important for device performance[34] and that are well described by the HSE06 functional.

We further characterize the electronic states responsible for the transition using the angular (l) and magnetic (m) quantum number-projected density of states. We find that the states involved in this transition are dominated by occupied mixture of *f*-orbitals ($m=-1, 1, 2, 3$) and unoccupied d_{yz} ($m=1$) orbitals-delocalized across Ce and Y ions. The *f*-*d* transition is allowed due to the selection rule $\Delta l = \pm 1$ ($l=2$ for *d* and $l=3$ for *f*-orbitals). In addition, $\Delta m = 0$ has to be satisfied for an allowed transition between *f*-*d* states.

We now compare the electronic and optical properties of other lanthanide-doped YAG materials. Figure 2(a) compares the transition strength for the lanthanide-doped YAG with that for pure YAG (see Fig. S2 for density of states in the supplementary material[35]). Interestingly, we observe the strongest transitions from occupied *f* to unoccupied *d* states for both the Ce and Pr dopants, which is consistent with experimental observations of luminescence in these materials.[3] Similar to Ce:YAG, the predicted transition energy of 4.13 eV for Pr:YAG agrees well with the experimental value of 3.9 eV.[36]

Furthermore, we establish the effects of co-doping with other lanthanides on the electronic and optical properties of LnCe:YAG. Fig. 2(b) shows the transition strength spectra for the co-doped LnCe:YAG, and Table I provides the energies and associated states for the most important optical transitions. We find that co-doping of Ce:YAG with La, Pr, Nd, Pm, and Gd red-shifts, while Lu blue-shifts the *d* to *f* transitions of 2.66 eV. The predicted shifts are consistent with the experimentally observed red shift for La and Gd and blue shift for Lu co-doping of Zhang *et al.*[19] However, due to exclusion of appropriate many-body effects, the quantitative value of the shifts are not in perfect agreement with experiments and can differ by about 0.3 eV.[37] For this series of lanthanide dopants (La, Pr, Nd, Pm, and Gd), the states dominating the optical transition are cerium *d* and *f* states. For the other co-dopants, the states dominating the optical transition appear to have strong contributions from the *f* and

TABLE I. Predicted major electronic transitions below 3 eV.

Name	*f*-*d* transition (eV)	*f*-*f* transition (eV)
LaCe	2.61,2.92	…
PrCe	2.59,2,91	…
NdCe	2.52,2.83	…
PmCe	2.44,2.75	…
EuCe	2.77,2.98	…
GdCe	2.2,2.54,2.92	…
TbCe	2.2,2.5,2.96	1.24,1.38,1.55
DyCe	2.96	2.16,2.2,2.46,2.83
HoCe	2.46,2.95	2.13,2.17,2.21
ErCe	1.67,2.19,2.96	1.29,1.37
TmCe	2.15,2.44,2.93,2.98	0.73,1.02
LuCe	2.68,2.97	…

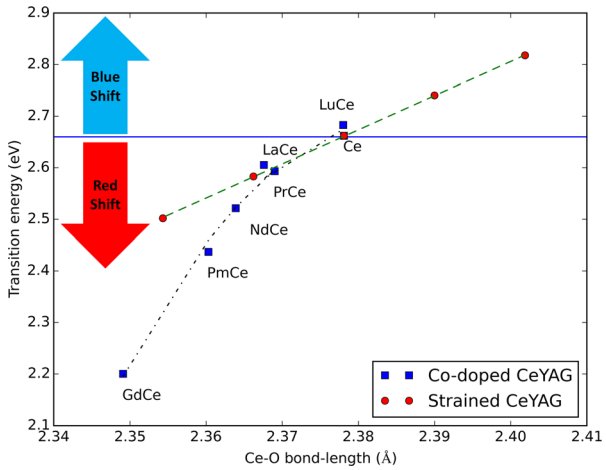

FIG. 3. Transition energies versus minimum in distribution of Ce-O bond lengths for volume strained and co-doped CeYAG. Both of the curves follow similar trends.

d orbitals of the lanthanide co-dopants. It is important to mention that the Ce-O bond-length decreases while the total volume expands in the case of Gd,Ce:YAG, which have been an open question for some time.[37] Here, by making use of the Ce-O bond length argument, it is possible to explain the red-shift in the co-doped system.

To identify the cause of the shift of the optical transition with co-doping across the lanthanide series, we calculate the charge of the ions using the Bader method[38] and determine the change in volume and in Ce-O bond length for the different co-dopants. We observe that the optical transition energy is correlated with the Ce-O bond length, which changes with the lanthanide co-dopant. To further elucidate this phenomenon, we show in Fig. 3 how the volumetric strain and the resulting change in Ce-O bond length affect the transition energies for the Ce:YAG system,[23,39] for a range of volumes comparable to that of the co-doped systems. The small compressive strains induced by the La, Pr, and Lu dopants result in a similar shift to that predicted for the volumetric strain. For the smaller Nd, Pm, and Gd dopants, we observe that the increased compressive strains enhances the red shift compared to the volume strain. We speculate that it could be attributed to the anisotropy of the dopant-induced strain.

Interestingly, we observe infrared transitions for the cases of doping with TbCe, ErCe, and TmCe. These dopant combinations result in available occupied and unoccupied *f* orbitals within the infrared range (see Fig. S3 for density of states in the supplementary material[35]). All other lanthanide co-doped systems only exhibit allowed *f-d* transitions. In the case of Er,Ce:YAG, experiments have already shown this material to be a high quantum efficiency up-conversion material.[7] Hence, due to the presence of these infrared transitions, which are related to quantum efficiency,[27] we suggest that Tb,Ce:YAG and Tm,Ce:YAG may also be useful up-conversion materials.

It is important to mention that YAG is prone to structural defects such as vacancies, interstitials, and impurities such as Si and Ca.[40] Effect of such defects on bonding environment and optical properties of YAG is our future work.

In conclusion, we have demonstrated that the semi-local exchange-correlation functional PBE accurately reproduces the structural and elastic properties of the YAG, while the hybrid exchange-correlation functional HSE06 can, in addition, accurately describe the experimental band gap and *f*-band positions. We predict that co-doping Ce:YAG with Tm or Tb results in infrared optical transitions very close or even lower in energy than ErCe:YAG; we thus anticipate that these materials will have quantum efficiencies comparable or higher than ErCe:YAG. Furthermore, we find that the lanthanide co-doping of Ce:YAG with La, Pr, Nd, Pm, Gd, and Lu results in a redshift of the optical transition frequency of Ce:YAG that is mainly attributed to strains of the bonding environment around the Ce-dopant. The transition strength methodology used here is directly applicable to more general problems involving, for instance, semiconductors, perhaps leading to better understanding of underlying optoelectronic phenomena. We believe that the findings of the work can be utilized in building systematics and making experimental samples with required material properties.

We gratefully acknowledge the support of the U.S. Army Research Office through Contract No. W911NF-12-1-0153. K.M. and R.G.H. were supported by the NSF under the CAREER Award No. DMR-1056587 and under Award No. ACI-1440547. This research used computational resources provided by the University of Florida Research Computing (http://researchcomputing.ufl.edu). We also thank Dr. Paul Holloway and Dr. David Tanner for helpful discussions.

[1]N. Wei, T. Lu, F. Li, W. Zhang, B. Ma, Z. Lu, and J. Qi, Appl. Phys. Lett. **101**(6), 061902 (2012).
[2]I. Shoji, S. Kurimura, Y. Sato, T. Taira, A. Ikesue, and K. Yoshida, Appl. Phys. Lett. **77**(7), 939 (2000).
[3]D. Haranath, H. Chander, P. Sharma, and S. Singh, Appl. Phys. Lett. **89**(17), 173118 (2006).
[4]S. Kobyakov, A. Kaminska, A. Suchocki, D. Galanciak, and M. Malinowski, Appl. Phys. Lett. **88**(23), 234102 (2006).
[5]J. X. Meng, K. W. Cheah, Z. P. Shi, and J. Q. Li, Appl. Phys. Lett. **91**(15), 151107 (2007).
[6]G. Zhu, X. Wang, H. Li, L. Pan, H. Sun, X. Liu, T. Lv, and Z. Sun, Chem. Commun. **48**(7), 958 (2012).
[7]Q. Wang, L. Su, H. Li, L. Zheng, X. Xu, H. Tang, X. Guo, D. Jiang, and J. Xu, Phys. Status Solidi A **208**(12), 2839 (2011).
[8]M. Pokhrel, G. A. Kumar, P. Samuel, K. I. Ueda, T. Yanagitani, H. Yagi, and D. K. Sardar, Opt. Mater. Express **1**(7), 1272 (2011).
[9]A. B. Munoz-García, E. Anglada, and L. Seijo, Intern. J. Quant. Chem. **109**(9), 1991 (2009).
[10]A. B. Munoz-García, J. L. Pascual, Z. Barandiarán, and L. Seijo, Phys. Rev. B **82**, 064114 (2010).
[11]W. Y. Ching, Y.-N. Xu, and B. K. Brickeen, Appl. Phys. Lett. **74**(25), 3755 (1999).
[12]A. J. Cohen, P. Mori-Sánchez, and W. Yang, Science **321**(5890), 792 (2008); J. Graciani, A. M. Márquez, J. J. Plata, Y. Ortega, N. C. Hernández, A. Meyer, C. M. Zicovich-Wilson, and J. F. Sanz, J. Chem. Theory Comput. **7**(1), 56 (2011); H. Guo, M. Zhang, J. Han, H. Zhang, and N. Song, Physica B: Condens. Matter **407**(12), 2262 (2012); S. Jiang, J. Chen, Y. Long, and T. Lu, J. Amer. Ceram. Soc. **95**(12), 3894 (2012); Z. Huang, J. Feng, and W. Pan, Solid State Sci. **14**(9), 1327 (2012).
[13]F. Fukudome, T. Tomiki, M. Kaminao, M. Fujisawa, Y. Tanahara, and T. Futemma, J. Phys. Soc. Jpn. **58**, 1801 (1989).
[14]Y. Ganaha, T. Tomiki, T. Shikenbaru, T. Futemma, M. Yuri, Y. Aiura, H. Fukutani, H. Kato, J. Tamashiro, Y. Miyahara, and A. Yonesu, J. Phys. Soc. Jpn. **62**(4), 1388 (1993).
[15]Y. Zhang, G. Kresse, and C. Wolverton, Phys. Rev. Lett. **112**(7), 075502 (2014); J. Paier, M. Marsman, K. Hummer, G. Kresse, I. C. Gerber, and J. G. Ángyán, J. Chem. Phys. **124**(15), 154709 (2006).
[16]M. Shishkin, M. Marsman, and G. Kresse, Phys. Rev. Lett. **99**(24), 246403 (2007).

[17]J. Heyd, G. E. Scuseria, and M. Ernzerhof, J. Chem. Phys. **124**(21), 219906 (2006); J. P. Perdew, M. Ernzerhof, and K. Burke, J. Chem. Phys. **105**(22), 9982 (1996).
[18]J. Heyd and G. E. Scuseria, J. Chem. Phys. **121**(3), 1187 (2004); J. Heyd, J. E. Peralta, G. E. Scuseria, and R. L. Martin, J. Chem. Phys. **123**(17), 174101 (2005).
[19]L. Zhang, H. Yang, P. De Han, L. X. Wang, and Q. T. Zhang, Mater. Sci. Forum. **663**, 129 (2011).
[20]G. Kresse and J. Furthmüller, Comput. Mater. Sci. **6**(1), 15 (1996); G. Kresse and J. Furthmüller, Phys. Rev. B **54**(16), 11169 (1996).
[21]P. E. Blöchl, Phys. Rev. B **50**(24), 17953 (1994).
[22]C. R. Varney, D. T. Mackay, A. Pratt, S. M. Reda, and F. A. Selim, J. Appl. Phys. **111**(6), 063505 (2012); Y.-D. Huh, Y.-S. Cho, and Y. R. Do, Bull. Korean Chem. Soc **23**(10), 1435 (2002).
[23]A. B. Munoz-García and L. Seijo, J. Phys. Chem. A **115**(5), 815 (2011).
[24]J. P. Perdew, K. Burke, and M. Ernzerhof, Phys. Rev. Lett. **77**(18), 3865 (1996).
[25]A. D. Becke, J. Chem. Phys. **98**(2), 1372 (1993).
[26]M. Gajdoš, K. Hummer, G. Kresse, J. Furthmüller, and F. Bechstedt, Phys. Rev. B **73**(4), 045112 (2006).
[27]F. Wooten, *Optical Properties of Solids* (Academic press, 2013).
[28]Ulrich Müller, *Inorganic Structural Chemistry* (Wiley, New York, 1993).
[29]L. Mezeix and D. J. Green, Int. J. Appl. Ceram. Tech. **3**(2), 166 (2006).
[30]M. A. Gülgün, W.-Y. Ching, Y.-N. Xu, and M. Rühle, Philos. Mag. B **79**(6), 921 (1999).
[31]Y. Isa, T. Tomiki, Y. Kadekawa, Y. Ganaha, N. Toyokawa, T. Miyazato, M. Miyazato, T. Kohatsu, H. Shimabukuro, and J. Tamashiro, J. Phys. Soc. Jpn. **65**, 1106 (1996).
[32]T. Tomiki, H. Akamine, M. Gushiken, Y. Kinjoh, M. Miyazato, T. Miyazato, N. Toyokawa, M. Hiraoka, N. Hirata, and Y. Ganaha, J. Phys. Soc. Jpn. **60**(7), 2437 (1991).
[33]C. W. Thiel, H. Cruguel, H. Wu, Y. Sun, G. J. Lapeyre, R. L. Cone, R. W. Equall, and R. M. Macfarlane, Phys. Rev. B **64**(8), 085107 (2001).
[34]P. Deák, B. Aradi, T. Frauenheim, E. Janzén, and A. Gali, Phys. Rev. B **81**(15), 153203 (2010).
[35]See supplementary material at http://dx.doi.org/10.1063/1.4929434 for density of states, bader charge, and volume dependence analysis.
[36]P. Dorenbos, R. Visser, C. W. E. Van Eijk, N. M. Khaidukov, and M. V. Korzhik, IEEE Trans. Nucl. Sci. **40**(4), 388 (1993).
[37]T. Y. Tien, E. F. Gibbons, R. G. DeLosh, P. J. Zacmanidis, D. E. Smith, and H. L. Stadler, J. Electrochem. Soc. **120**(2), 278 (1973).
[38]G. Henkelman, A. Arnaldsson, and H. Jónsson, Comput. Mater. Sci. **36**(3), 354 (2006).
[39]A. B. Muñoz-García, J. L. Pascual, Z. Barandiarán, and L. Seijo, Phys. Rev. B **82**(6), 064114 (2010).
[40]M. M. Kuklja and R. Pandey, J. Amer. Ceram. Soc. **82**(10), 2881 (1999); M. M. Kuklja, J. Phys.: Condens. Matter **12**(13), 2953 (2000).